# Texture-based Segmentation of High-Resolution Remotely Sensed Imagery for Identification of Fuzzy Objects

Arko Lucieer*, Peter Fisher** & Alfred Stein*

* International Institute for Geo-Information Science and Earth Observation (ITC),
Department of Earth Observation Science,
P.O. Box 6, 7500 AA Enschede, The Netherlands
Telephone: +31 (0)53 4874256, Fax: +31 (0)53 4874335
Email: lucieer@itc.nl, stein@itc.nl

** University of Leicester,
Department of Geography,
Leicester, LE1 7RH, United Kingdom
Telephone: +44 (0)116 2523839, Fax: +44 (0)116 252 3854
Email: pff1@le.ac.uk

## Abstract

In this study, we discuss a supervised texture-based image segmentation algorithm. We apply this algorithm to airborne high-resolution elevation (LiDAR) and multi-spectral imagery (CASI) of a coastal area on the northwest coast of England. Texture is modelled with the joint distribution of the Local Binary Pattern (*LBP*) operator and local variance. Spatial objects are derived from the imagery based on a supervised hierarchical splitting segmentation algorithm. Additionally, information on thematic and spatial uncertainty of the objects is derived. This information is needed for identification of objects with indeterminate boundaries or fuzzy objects.

## 1. Introduction

Recent research on remote sensing classification has focused on modelling and analysis of classification uncertainty. Both fuzzy and probabilistic approaches have been applied (Foody, 1996; Hootsmans, 1996; Canters, 1997; Fisher, 1999; Wel, 2000; Zhang and Foody, 2001). Much of this research, however, focused on uncertainty of spectral classification at a pixel-by-pixel basis, ignoring potentially useful spatial information between pixels. An object-based approach instead of a pixel-based approach may be helpful in reducing uncertainty. Additionally, interpretation of uncertainty of real world objects may be more intuitive than interpretation of uncertainty of individual pixels.

Object-oriented approaches to remotely sensed image processing have become popular with the growing amount of high-resolution satellite and airborne imagery. Several studies have shown that segmentation techniques can help to extract spatial objects from an image (Gorte and Stein, 1998). Segmentation differs from classification, as spatial contiguity is an explicit goal of segmentation whereas it is only implicit in classification. Uncertainty, however, occurs in any segmented image and can affect further image processing. In particular, in areas where objects with indeterminate boundaries (so-called fuzzy objects) dominate an indication of segmentation uncertainty is important.

A straightforward approach to identify fuzzy objects is to apply a (supervised) fuzzy *c*-means classification, or similar soft classifier. This classifier gives the most likely class for a pixel, and also possibility values of belonging to any other class. It does not, however, take spatial correlation between pixels into account, also known as pattern or texture.

Cheng and Molenaar (2001) proposed a fuzzy analysis of dynamic coastal landforms. They classified the beach, foreshore and dune area as fuzzy objects based on elevation data using a semantic import model. Some classification errors, however, are likely to occur when using elevation as diagnostic information alone. For example, an area of low elevation behind the foredune is classified as beach, whereas it is almost certainly an area of sand removal by the wind like a blowout or an interdune area. These types of errors can be prevented by using spatial or contextual information, i.e. by looking at morphometry or landforms. Cheng *et al.* (2002) and Fisher (2002) propose a novel method of multi-scale analysis for allocating fuzzy memberships to morphometric classes. This technique can be used to model objects, which are vague for scale reasons. The morphometry classes modelled at different scale levels are: channel, pass, peak, pit, plane, and ridge. Although this analysis fails to identify positions of dunes, it is possible to identify dune ridges and slacks and to monitor their changing positions.

In this study, we are interested in both vegetation and landforms as characterization of coastal land units. To identify these units we argue that texture is of utmost importance. A description of texture reflects the spatial structure of both elevation and spectral data and is therefore indispensable in classifying an area into sensible geographical units. The aim of this study is to present a supervised texture-based image segmentation technique that identifies objects from high-resolution elevation and multi-spectral airborne imagery. It is applied to a coastal area in northwest England. This paper builds on work of Lucieer and Stein (2002) and further explores the use of texture and generation of thematic and spatial object uncertainty in image segmentation to identify fuzzy objects.

## 2. Study area and data

### 2.1 The Ainsdale Sands

The study area (6 $km^2$) is on the coast of northwest England named Ainsdale Sands. The Ainsdale Sand Dunes National Nature Reserve (NNR) totals 508 ha and forms part of the Sefton Coast, the finest dune system on the northwest coast of England. The NNR is within the coastal Special Protection Area. It is also within the Sefton Coast candidate Special Area of Conservation. The NNR contains a range of habitats, including intertidal sand flats, embryo dunes, high mobile yellow dunes, fixed vegetated dunes, wet dune slacks, areas of deciduous scrub and a predominantly pine woodland. Key species include dune helleborine, pendulous flowered helleborine, sand lizard, natterjack toad, great crested newt, and red squirrel. The red squirrel is the only native squirrel in the British Isles. Widespread in Britain at the turn of the century, it has since shown a dramatic decline due to the loss and fragmentation of habitat, disease and, in particular, competition from the larger introduced grey squirrel. To aid the red squirrel in the long term it is important that appropriate habitat management is practiced to allow red squirrels to survive in areas that would otherwise be taken over by greys.

There are 460 species of flowering plants recorded, including 33 locally or regionally rare species. The shore holds important wintering populations of various waders and gulls.

Management of this area consists of extending the area of open dune habitat through the removal of pine plantation from the seaward edge of the NNR, maintaining and extending the area of fixed open dune by grazing with Herdwick sheep and progressively creating a more diverse structure within the remaining 115 ha pine plantation with associated benefits for wildlife (Ainsdale Sand Dunes NNR, 2003). Therefore, mapping of this coastal area is important for protection and management of the environment as a major and threatened habitat type and as a defence against coastal flooding.

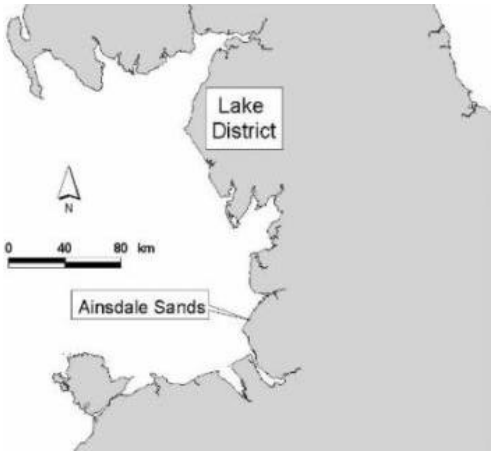


Figure 1. Location of the study area in northwest England north of Liverpool
(Source: Fisher, 2002)

## 2.2 LiDAR and CASI imagery

In 1999, 2000 and 2001 the Environment Agency, UK, collected high-resolution digital elevation models (DEM) by LiDAR, and simultaneously, acquired hyper-spectral Compact Airborne Spectral Imager (CASI) imagery (one flight each year). The aircraft is positioned and navigated using Global Positioning Satellite (GPS) corrected to known ground reference points. The aircraft flies at approximately 800 m above ground level. A scanning mirror allows a swath width of approximately 600 m to be surveyed during a flight. Individual measurements are made on the ground at 2 m intervals for LiDAR and 1 m resolution for the CASI sensor allowing a highly resolved model of the terrain to be generated. In this study, the imagery of 2001 is used. These images, geometrically corrected by the Environment Agency, are spatial composites of multiple flight strips. The area covered by these images is approximately 6km$^2$. Figure 2A displays a grey scale image of band 12 (Near Infrared) of the CASI image. Figure 2B shows a 3D hill-shaded model of the LiDAR DEM of the study area.

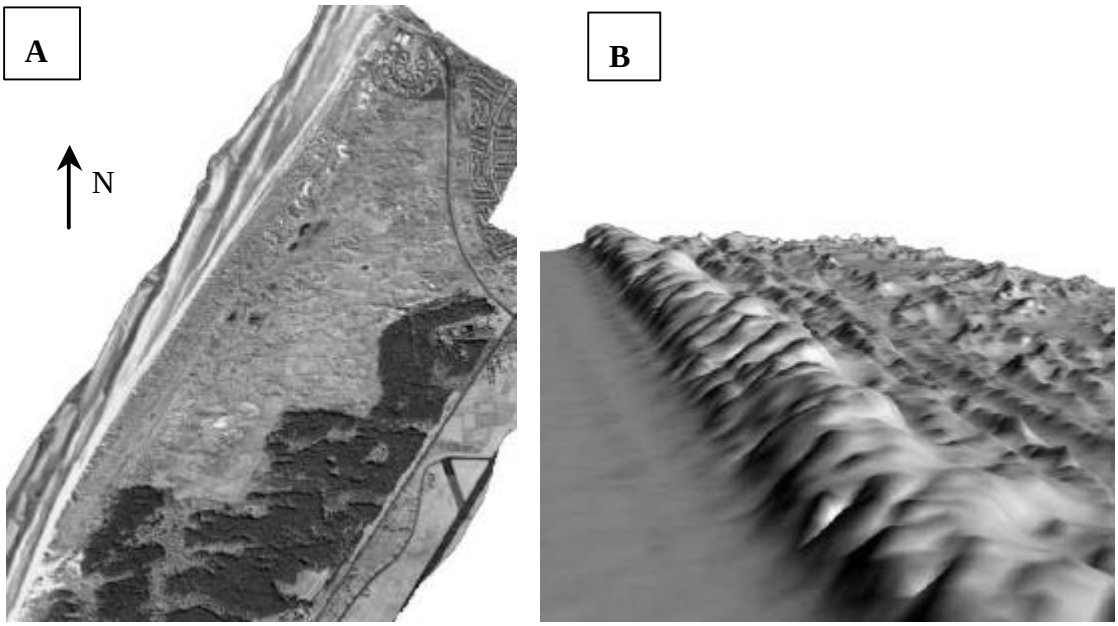

Figure 2. A: Band 12 (NIR) of the 1 m resolution CASI image of the Ainsdale Sands. B: 3D view of the 2 m resolution LiDAR DEM of the same area with the foredune clearly visible.

## 2.3 Coastal land units

In table 1 we distinguish the mapping units in the study area based on the information content in the LiDAR and CASI imagery and considering the required mapping units for management of the area. Detailed mapping of these units is required, because knowledge about the location and dynamics of these object types is important for monitoring the unique habitats in this area, as well as, the coastal defence against flooding.

We propose a hierarchical object structure with a distinction between land cover classes and land form classes. At the finest level, classes have diagnostic properties of both land cover and landform. These objects are unique because of their combined form and vegetation properties. It is important to distinguish between land cover and landform, because we cannot derive evidence for object identification from one type of data alone. Landform properties are extracted from digital elevation, the LiDAR DEM of the area. Land cover is obtained from spectral information from the CASI imagery. The objects proposed here have a fuzzy nature. Transition zones between objects occur and it is hard or even impossible to determine crisp boundaries between these objects. Therefore, information on thematic and spatial uncertainty is required to identify these objects. In the next section, we describe methods for the extraction of these objects that provide additional information about their uncertainties.

Table 1. Hierarchical structure of coastal mapping units

| | Elevation / Land form | Land cover / Vegetation | Coastal mapping units |
|---|---|---|---|
| Beach | Beach flat | Wet Sand<br>Dry Sand | Wet beach<br>Dry beach |
| | | | |
| Dune field | Foredune<br><br>Dune (parabolic)<br>Dune ridge<br><br>Dune trough<br>Blowout | Woodland (Pine tree)<br>Grass (Marram)<br>Willow Shrub<br><br>Sand | Vegetated foredune<br><br>Woodland dune<br>Woodland dune trough<br>Vegetated dune<br>Bare dune<br>Vegetated dune ridge<br>Vegetated dune trough<br>Fossil blowout (vegetated)<br>Active blowout |

# 3. Methods

## 3.1 Texture

Regions with similar reflection can easily be identified as objects on a remote sensing image. The presence of texture makes it more complicated. Without agreement on a formal definition of texture, a major characteristic is the repetition of a pattern or patterns over a region. The pattern may be repeated exactly, or as a set of small variation, possibly as a function of position. There is also a random aspect to texture, because size, shape, colour and orientation of pattern elements (sometimes called textons) can vary over the region.

We would like to be able to describe texture (texture descriptions are measurements which characterize a texture) and then to classify it (classification is attributing the correct class label to a set of measures) or perhaps to segment an image according to its texture content. Texture measures can be split into structural (transform-based), statistical and combination approaches. Well-known structural approaches are the Fourier and Wavelet transform. We can use several measures to describe these transforms, including entropy, energy and inertia (Nixon, 2002). The most well known statistical approach toward texture description is the grey level co-occurrence matrix (GLCM) (Haralick *et al.*, 1973). The co-occurrence matrix contains elements that are counts of the number of pixel pairs for specific brightness levels, when separated by some distance and at some relative inclination. Other well-known texture descriptors are Markov random fields (GMRF), Gabor filter, fractals and wavelet models. A comparative study of texture classification is given in (Randen and Husoy, 1999).

## 3.2 Texture model – the Local Binary Pattern Operator (LBP)

The degree of computational complexity of most texture models is too high. Therefore, Randen and Husoy (1999) conclude in their recent comparative study that a direction for future research is the development of powerful texture measures that can be extracted and classified with a low computational complexity. A relatively new and simple texture model is

the local binary pattern operator (*LBP*) (Pietikäinen *et al.,* 2000; Ojala *et al.* 2002). It is a theoretically simple yet efficient multi-resolution approach to grey scale and rotation invariant texture classification based on local binary patterns and nonparametric discrimination of sample and prototype distributions.

Ojala *et al.* (2002) derive *LBP* by defining texture $T$ in a local neighbourhood of a grey scale image as the joint distribution of grey levels of $P$ ($P>1$) image pixels

$$T = t(g_c, g_0, ..., g_{P-1}) = t(g_c, g_P) \quad (1)$$

where $g_c$ corresponds to the value of the centre pixel ( $p_c$ ) of the local neighbourhood and $g_i$ corresponds to the value of a pixel ( $p_i$, where $i = 0, ..., P-1$) in the neighborhood of $p_c$. In this study, we apply a circle of radius $R$ with $P$ equally spaced pixels that form a circularly symmetric neighbourhood set (figure 3B). If the coordinates of $p_c$ are $(k,l)$, then the coordinates of the neighbouring pixels in a circular neighbourhood are given by

$$p_i(k,l) = p_i(k - R\sin(2p\,i/P), l + R\cos(2p\,i/P)) \quad \text{for } i = 0, ..., P-1 \quad (2)$$

Common combination of $P$ and $R$ are: 4-1 (corresponding to the 4 adjacent neighbours), 8-1 (corresponding to the 8 adjacent neighbours, or a 3x3 kernel), 16-2 and 24-3. Duplicate pixels are ignored in the neighbourhood set.

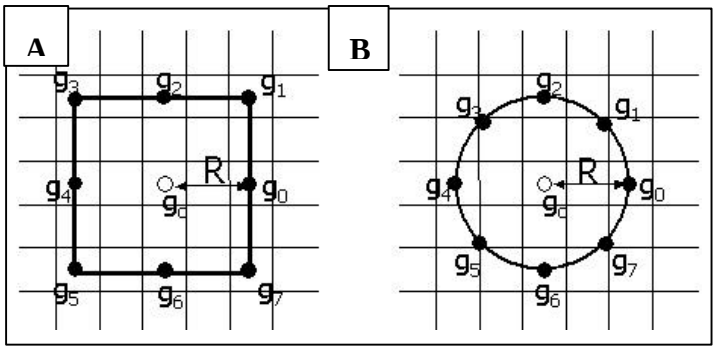


Figure 3. A: a square and B: circular pixel neighbourhood set for $P = 8$ and $R = 2$ (source: Texture Analysis, University of Oulu, Finland, 2003).

Invariance with respect to the scaling of pixel values or illumination differences is achieved by considering just the signs of the differences instead of their exact values

$$T \approx t(s(g_0 - g_c), s(g_1 - g_c), ..., s(g_{P-1} - g_c)) \quad (3)$$

where

$$s(x) = \begin{cases} 1, x \geq 0 \\ 0, x < 0 \end{cases} \quad (4)$$

Ojala *et al.* (2002) found that not all local binary patterns describe properties of texture well. They introduce a uniformity measure $U$ to define 'uniform' patterns. $U$ corresponds to the number of spatial transitions or bitwise 0/1 changes in the pattern.

$$U(LBP_{P,R}) = \sum_{i=1}^{P} \left| s(g_i - g_c) - s(g_{i-1} - g_c) \right| \quad (5)$$

where

$$g_P = g_0 \quad (6)$$

Patterns that have uniformity values of at most 2 are designated as uniform resulting in the following operator for grey scale and rotation invariant texture description

$$LBP_{P,R}^{riu2} = \begin{cases} \sum_{i=0}^{P-1} s(g_i - g_c) & \text{if } U(LBP_{P,R}) \le 2 \\ P+1 & \text{otherwise} \end{cases} \quad (7)$$

The $LBP_{P,R}^{riu2}$ operator thresholds the pixels in a circular neighbourhood of $P$ equally spaced pixels on a circle of radius $R$, at the value of the centre pixel. The $LBP_{P,R}^{riu2}$ operator allows for detecting uniform patterns for any quantization of the angular space and for any spatial resolution. It allows for combining multiple operators, $LBP_{P,R}^{riu2}$ with different neighbourhood sets (i.e. different values for $P$ and $R$), for multi-resolution analysis. $P$+1 uniform binary patterns can occur in a circular symmetric neighbourhood set of $P$ pixels. Equation 7 assigns a unique lable to each of the patterns, corresponding to the number of '1' bits in the pattern. The non-uniform patterns are grouped under one label, $P$+1.

Most approaches to texture classification or segmentation assume that training samples and unknown samples are identical with respect to spatial scale orientation and grey scale properties. This is often not the case, however, real world textures can occur at arbitrary spatial resolutions, rotations and illumination conditions. The $LBP_{P,R}^{riu2}$ operator is very robust in terms of grey scale variations, since the operator is by definition invariant against any monotonic transformation of the grey scale. The operator is an excellent measure of the spatial structure of local image texture, but by definition, it discards the other important property of local image texture, i.e. contrast. Therefore, the performance of $LBP_{P,R}^{riu2}$ can be further enhanced by combining it with a rotation invariant variance measure that characterizes the contrast of local image texture. The variance is defined as

$$\hat{s}_g^2 = \frac{1}{P} \sum_{i=0}^{P-1} (g_i - \hat{m}_g)^2 \quad (8)$$

where

$$\hat{m}_g = \frac{1}{P} \sum_{i=0}^{P-1} g_i \quad (9)$$

Most approaches to texture analysis quantify texture measures by single values (means, variances, entropy, etc.). However, much important information contained in the distributions of feature values might be lost. In this study, the final texture feature is the histogram of $LBP_{P,R}^{riu2}$ occurrence, computed over an image or a region of an image, or the joint distribution

of the two complementary $LBP_{P,R}^{riu2}$ and $\hat{s}_g^2$ operators. The joint distribution of ($LBP_{P,R}^{riu2}$, $\hat{s}_g^2$) is approximated by a discrete two-dimensional histogram of size *P+1 x b*, where *P* is the number of neighbours in a circular neighbourhood and *b* is the number of bins for $\hat{s}_g^2$. Ojala *et al.* (2002) show that this is a powerful tool for rotation invariant texture classification. The number of bins used in quantization of the feature space plays a crucial role. Histograms with too modest a number of bins fail to provide enough discriminative information about the distributions, however, if we go to the other extreme the number of entries per bin is very small and histograms become sparse and unstable. In this study, following Ojala *et al.* (1996), the feature space is quantized by computing the total feature distribution of ($LBP_{P,R}^{riu2}$, $\hat{s}_g^2$) for the whole image. This distribution is divided into 32 bins having an equal number of entries.

In classifying texture, we evaluate the (dis)similarity of sample and model histograms as a test of goodness-of-fit using a nonparametric statistic, the log-likelihood ratio statistic, also known as the *G*-statistic (Sokal and Rohlf, 1987). Here, the sample is a histogram of the texture measure distribution of an image window. The model is a histogram of a reference image window of a particular class. By using a nonparametric test we avoid making any, possibly erroneous, assumptions about the feature distributions. The value of the *G*-statistic indicates the probability that two sample distributions come from the same population: the higher the value, the lower the probability that the two samples are from the same population. The more alike the histograms are, the smaller is the value of *G*.

It should be noted that the window size should be appropriate for the computation of the texture features. However, as we consider windows of increased size, the probability that regions contain a mixture of textures is increased. This can bias the comparison, since the reference textures contain only features of individual patterns. On the other hand, if the window size is too small it is impossible to calculate a texture measure. Within this constraint, it is impossible to define an optimum size for segmenting the entire image, therefore, classifying regions of a fixed window size is inappropriate (Aguado *et al.*, 1998). Alternatively, a top-down hierarchical segmentation process, as discussed in the next section, offers a very suitable framework for classifying image regions based on texture.

## 3.3 Texture based image segmentation

Split-and-merge segmentation consists of a region-splitting phase and an agglomerative clustering (merging) phase (Haralick and Shapiro, 1985; Horowith and Pavlidis, 1976 and Lucieer and Stein 2002). In the approach of Lucieer and Stein (2002), the image is initially considered as a block of pixel values with mean vector and covariance matrix. This block is split into four sub-blocks characterized by vectors of mean pixel values and covariance matrices. To define homogeneity, they consider a threshold for the mean and thresholds for the covariance matrix. These values are chosen in advance and kept constant during segmentation. Heterogeneous sub-blocks are split recursively until homogeneity occurs or a minimum block size is reached. The resulting data structure is a regular quadtree. In the clustering phase, adjacent block segments are merged if the combined object is homogeneous. The homogeneity rules are applied in a similar way. Texture is not taken into account in this approach.

Ojala and Pietikäinen (1999) apply a similar unsupervised split-and-merge segmentation with

splitting and merging criteria based upon the ($LBP^{riu2}_{P,R}$, $\hat{s}^2_g$) texture measure (section 3.2). Objects derived with unsupervised segmentation have no class labels. Class labels can be assigned in a separate labelling or classification stage. Supervised segmentation uses explicit knowledge about the study area to train the segmentation algorithm on reference texture classes. In such an approach, segmentation and classification are combined and objects with class labels are obtained.

Aguado *et al.* (1998) introduce a segmentation framework with a top-down hierarchical splitting process based on minimizing uncertainty. In this study, we combine the ($LBP^{riu2}_{P,R}$, $\hat{s}^2_g$) texture measure as describe in section 3.2 and the segmentation/classification framework as suggested by Aguado *et al.* (1998). Similar to split-and-merge segmentation each square image block in the image is split into four sub-blocks forming a quadtree structure. The criterion used to determine if an image block is divided is based on a comparison between the uncertainty of the block and the uncertainty of the sub-blocks. Uncertainty provides a measure that reflects the potential classification ambiguity of image regions.

To obtain optimum image segmentation, we divided the image such that classification confidence is maximized, and hence uncertainty is minimised, where uncertainty is defined as the ratio between the similarity values, computed from an image block, of the two most likely reference textures. These textures are histograms of ($LBP^{riu2}_{P,R}$, $\hat{s}^2_g$) of characteristic regions in the image. To test for similarity between an image block texture and a reference texture we apply the *G*-statistic described in section 3.2. Uncertainty *U* is defined as

$$U = \frac{G_2}{G_1} \tag{3.10}$$

where $G_1$ is the lowest *G* value of all classes (highest similarity) and $G_2$ is the second lowest *G* value. *U* is close to one if $G_1$ and $G_2$ are very similar. In this case, the decision of classifying the region is vague. The uncertainty in classification decreases if the difference between these two texture similarities increases. The subdivision of each image block is based on this uncertainty criterion. An image block is split into four sub-blocks if

$$U_B \cdot 4 > U_{SB1} + U_{SB2} + U_{SB3} + U_{SB4} \tag{3.11}$$

where the left side of equation 11 defines uncertainty obtained when the sub-blocks are classified according to the class obtained by considering the whole block (*B*). The right side of equation 11 defines uncertainty obtained if the sub-blocks (*SB1, SB2, SB3* and *SB4*) are classified by the classes obtained by the subdivision. Thus, the basic idea is to subdivide an image block only if it is composed of several textures. Additionally, classification is always uncertain at the boundaries of textures because the image block contains a mixture of textures. Accordingly, we subdivide blocks that have at least one neighbouring region of a different class (Aguado *et al.*, 1998). Finally, we obtain a partition of the image of objects labelled according to the reference texture classes.

The building blocks of each of the objects give information about the objects' uncertainties. We use the measure $U_B$ to depict the ambiguity with which a block is assigned a class label.

This gives us information about the thematic uncertainty of the building blocks. The spatial distribution of building block uncertainty within an object gives information about spatial uncertainty. We expect high uncertainty values in the boundary blocks within objects, because of mixed textures or transition zones.

## 3.4 Texture example

To illustrate the problem of classifying regions of different texture we use an image (512 X 512 pixels) with a composition of photos of five different textures (figure 4A). Each of these classes is unique in terms of their texture. It shows that the human visual system not only distinguishes image regions based on grey scale or colour, but also on pattern. A pixel-based classifier does not take into account texture or spatial information. This is shown in figure 4B, which gives the result of a (pixel based) supervised fuzzy *c*-means using a Mahalanobis distance measure and an overlap parameter of 2.0 with five classes (Bezdek, 1981). We selected five regions of 30 by 30 pixels in the centres of the texture regions to train the classifier. Figure 4B shows that, although the patterns are still visible, no clear spatial partition of classes is found.

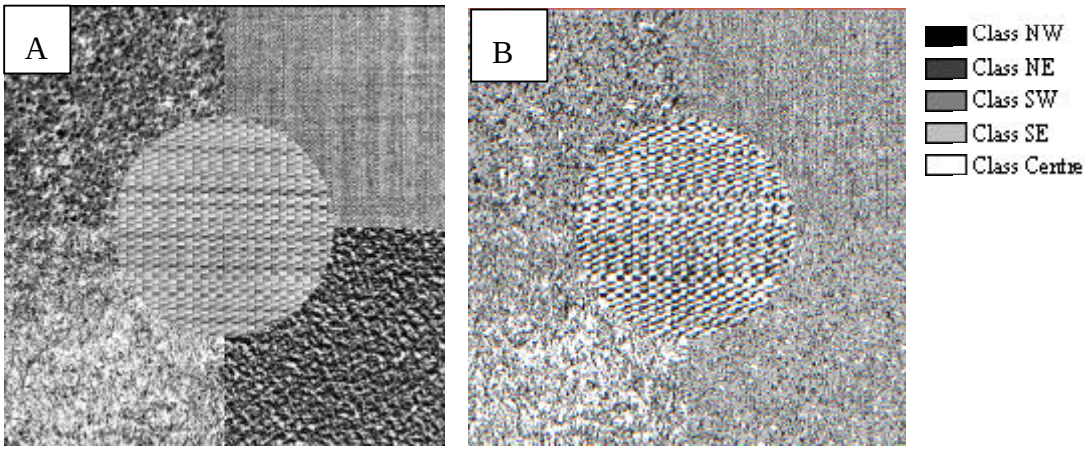


Figure 4. A: Artificial composition of five different natural textures. B: Result of a pixel based supervised fuzzy c-means classifier.

Figure 5 gives the results of two segmentations of figure 4A.Figure 5A shows that a split-and-merge segmentation (see section 3.3) without texture characterization cannot identify regions of homogeneous texture. It should be noted that this approach is unsupervised, i.e. no reference data is used to train the algorithm (Lucieer and Stein, 2002). Random grey values are used to depict different objects. Figure 5B shows that a much better segmentation of figure 4A occurs if texture is incorporated into segmentation, applying the supervised texture-based segmentation algorithm proposed by Ojala and Pietikäinen (1999) (see section3.3).

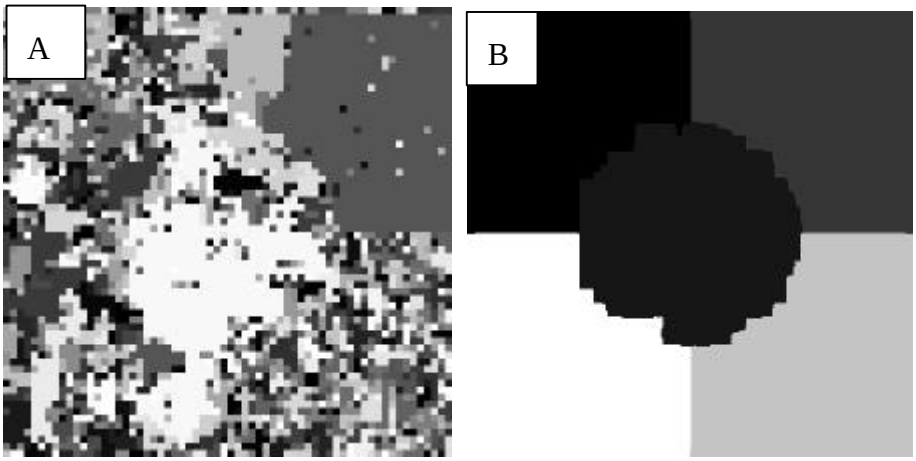

Figure 5. A: unsupervised split-and-merge segmentation of figure 4A based on mean and variance. B: unsupervised split-and-merge segmentation based on texture distributions.

In figure 6 the results of a supervised texture-based segmentation of figure 4A are shown, applying the uncertainty criteria of Aguado *et al.* (1998) (see section 3.3). We selected five references regions of 40x40 pixels in the image, corresponding to the five different texture classes (similar to the supervised fuzzy *c*-means classification). Values for *P* and *R* are 8 and 1 respectively (corresponding to the 8 adjacent neighbours). Figure 6A shows the segmented objects with their corresponding class label. In figure 6B uncertainty values for each of the objects' building blocks are given. Class NE is segmented with lowest uncertainty values, between 0.3 and 0.4. The centre class is segmented with uncertainty values between 0.4 and 0.5. Class SW is segmented well, but with a higher uncertainty, between 0.5 and 0.7. Ambiguity of this class occurs with class SE. Class NW is segmented well, but with high uncertainty values between 0.5 and 0.75. In class NW a cluster of small objects is classified as class SW. The building blocks of these objects show uncertainty values of 0.95 and higher, meaning that the classification ambiguity in these areas is very high. Ambiguity of this class occurs with class SE. The main area of Class SE is segmented well, but the objects show the highest uncertainty values in the image (between 0.6 and 1.0). In this class, small objects are classified as class NW, SE and Centre. Block uncertainty is higher than 0.94 for these objects. This can be explained by the fact that this type of texture is very irregular, i.e. its pattern is not repetitive and the reference area does not fully represent the whole texture area. In addition, all small blocks at the boundaries of textures show high (>0.9) uncertainties, because they contain mixtures of different textures.

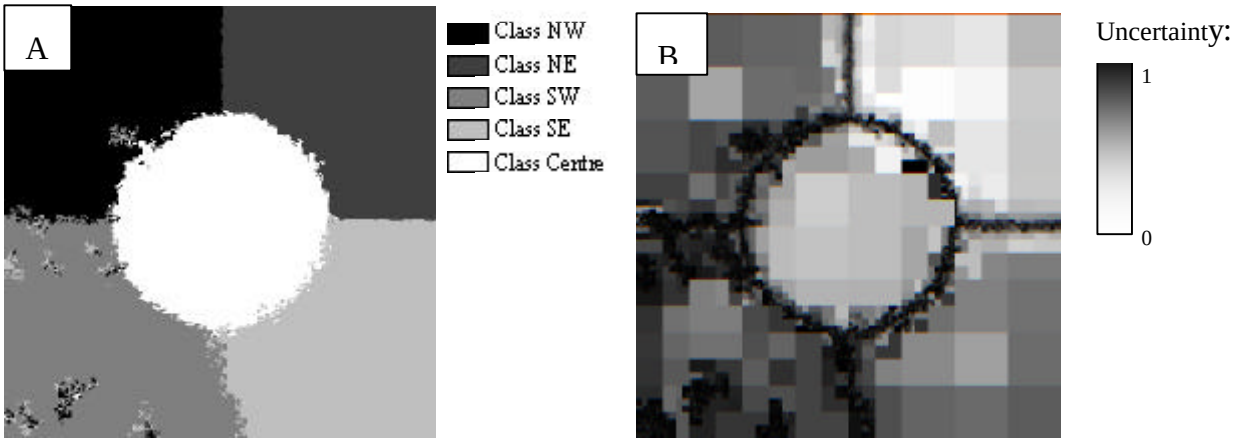

Figure 6. A: Supervised texture based segmentation of figure 4A with five reference classes. B: Related uncertainty for all object building blocks.

## 4. Results

### 4.1 Segmentation of LiDAR DEM

Figure 7 shows the result of a supervised segmentation of a 512 by 512 pixel subset of the LiDAR DEM of the study area. Four reference areas of 50 by 50 pixels were selected for training. Again, values for *P* and *R* are 8 and 1 respectively. Figure 7A shows the segmented objects with class labels and figure 7B shows the corresponding uncertainty values. Woodland gives a unique response in the LiDAR image. Its texture is different from other classes. Therefore, we classified woodland as one of the landform classes in this image. The woodland area is segmented well, with low uncertainty values ranging from 0.02 to 0.35. Uncertainty values increase at the border of the woodland area. Fieldwork showed that zones of willow trees occurred at the border of the main pine woodland area, which because of their slightly different texture explain the higher uncertainty. Dune slacks and blowouts are very similar in form. Blowouts are active, however, and not vegetated. Dune slacks are often stable, because they are vegetated. These differences do not show in texture differences in the LiDAR image. Therefore, these units are segmented as one class type, dune slacks. The core of these areas is segmented well, with uncertainty values between 0.2 and 0.5. The boundaries of these objects, however, show uncertainty values of 0.8 and higher. These high uncertainty values are explained by the fact that dune slacks show a transition to dune. No crisp boundary can be defined between these objects types. High uncertainty values depict that there is a transition zone between objects and that these objects have a fuzzy nature. Furthermore, figure 7 shows that no distinction could be made between the foredune and the inland dune field. These areas have similar image textures and, therefore, are segmented as one class. The (steep) foredune shows, as expected, a short transition zone to beach, depicted by high uncertainty values (>0.8). The dune area is segmented with low uncertainty values (<0.4) except for the transition zones with the dune slacks. In the southwest and centre part of the image, small objects (with uncertainty values of 0.95) are classified as beach. This can be explained by the fact that this area is an active flat and bare sand area, with similar texture to the beach. The beach flat is classified early in the segmentation process, as can be concluded from the large building blocks. Uncertainty related to the classification of these building blocks varies between 0.1 and 0.5. Within the beach area, highest uncertainty occurs in areas where the sand is wet and shows a different texture from dry sand.

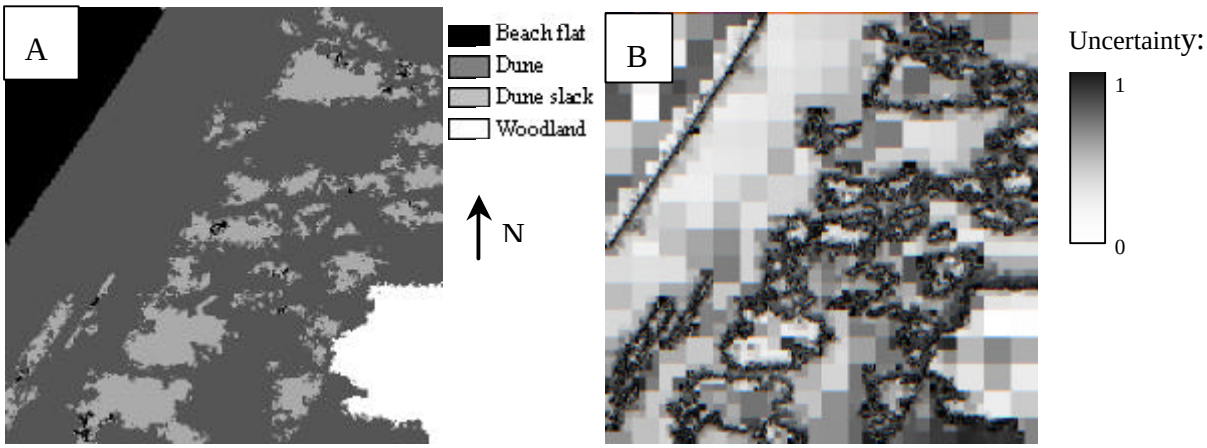

Figure 7. A: Classification result of supervised texture based segmentation of the LiDAR DEM with four reference land form classes. B: Related uncertainty for all object building blocks.

## 4.2 Segmentation of CASI image

In figure 8, the results of the segmentation of the CASI image are shown. The image is resampled to a resolution of 2 m to match the resolution of the LiDAR image. Again, a subset of 512 by 512 pixels is used for segmentation. Figure 8A shows the segmentation result of four land cover types. Four reference areas of 50 by 50 pixels were selected to train the algorithm. Values for *P* and *R* are 8 and 1 respectively. The woodland area in the southeast corner of the image is correctly segmented with uncertainty values between 0.1 and 0.5 (figure 8B). The northeastern corner of the image and small objects in the northern part of the image are also segmented as woodland. However, fieldwork showed that no woodland is found in this area. The area is characterized by a chaotic pattern of dune slacks and dune ridges with a mixture of vegetation types and no homogeneous textures can be found. This is depicted by high uncertainty values (>0.7) in the area. The main part of the dune field is classified as willow shrub land. Fieldwork showed that marram grass is mainly found on the foredune and on the highest parts of the dune ridges in the dune field. Only a few small patches of marram grass are shown in figure 8A in the foredune area. Willow shrub is found all over the dune field, but mainly in the dune slacks. Image texture for these two classes, however, is very similar. Marram grass fields are characterized by a mixture of grass and sand; willow shrub areas are characterized by a mixture of baby willow shrubs and sand or low grass. High uncertainty values (higher than 0.7 in the dune field and higher than 0.95 in the foredune and dune ridge areas) in figure 8B confirm the ambiguity between these two classes. The sand cover on the beach is correctly segmented, because of its unique texture. Uncertainty values are lower than 0.2. Again, there is a short transition zone from the foredune to the beach with a decreasing marram grass coverage. This zone is depicted by uncertainty values of 0.95 and higher.

## 5. Discussion & Conclusions

In this study, texture is used to segment a LiDAR elevation model and a CASI image band into objects. Additionally, absolute elevation and reflection values might be used in segmentation to improve results. Errors like classifying beach objects inside the dune field are might be prevented by taken into account this information.

The resolution of the neighbourhood set affects the segmentation result. In this study, we

used a neighbourhood set of the nearest eight neighbouring pixels ($P$=8, R=1). A multi-resolution approach with different combinations of $P$ and $R$ might describe textures in a better way. In future research we will assess the effect of different neighbourhood sets on the segmentation result. Additionally, we will look into a multi-spectral approach with a multi-variate $LBP^{riu2}_{P,R}$ and ($LBP^{riu2}_{P,R}$, $\hat{s}^2_g$) descriptor. Multiple CASI bands will be used in the texture description and might provide a more accurate texture model.

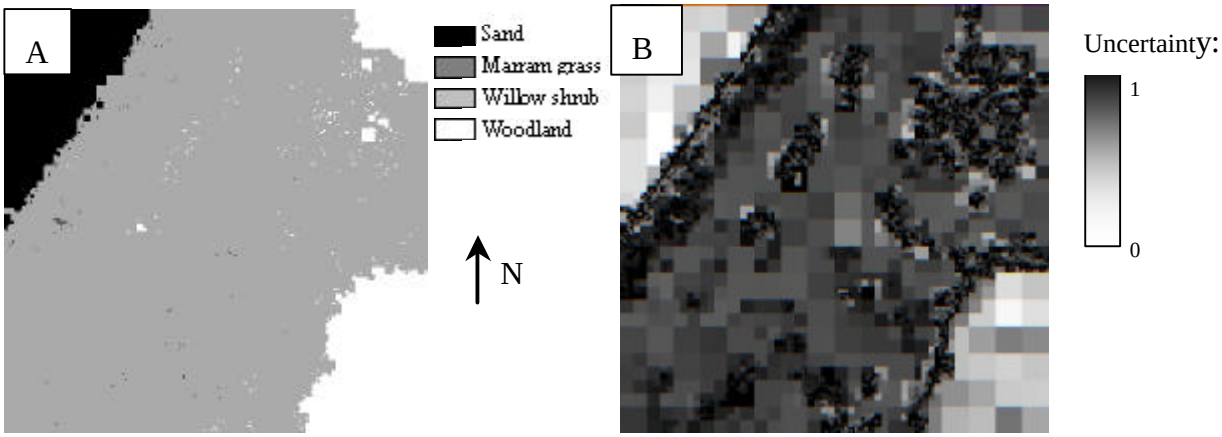


Figure 8. A: Classification result of supervised texture based segmentation of band 12 of the CASI image with four reference land cover classes. B: Related uncertainty for all object building blocks.

In this paper, we propose a supervised segmentation algorithm to derive labelled objects from remotely sensed imagery based on image texture. Image texture is modelled with the joint distribution of the Local Binary Pattern operator (*LBP*) and local variance. Additionally, we focus on the generation of thematic and spatial object uncertainty. For each of the objects' building blocks, uncertainty values are calculated to depict class ambiguity. Spatial distribution of building block uncertainty inside objects gives us information about spatial uncertainty of objects. Transitions zones between object classes are depicted by high uncertainty values. This study shows that uncertainty values provide us with invaluable information to identify transition zones between (fuzzy) objects and to identify areas with ambiguous classification.

## References


Ainsdale Sand Dunes NNR, English Nature National Natural Reserves. 2003. Website http://www.english-nature.org.uk. Last accessed: 24 January 2003.

AGUADO A.S., MONTIEL E., AND M.S. NIXON. 1998. Fuzzy image segmentation via texture density histograms. EU project Nr. ENV4-CT96-0305 - Fuzzy Land Information from Environmental Remote Sensing (FLIERS) Final Report, 1998.

BEZDEK, J. 1981, Pattern Recognition with Fuzzy Objective Function Algorithms, Plenum Press, New York.

CANTERS F. 1997. Evaluating the uncertainty of area estimates derived from fuzzy land cover classification. *Photogrammetric Engineering & Remote Sensing*, 63(4):403-414.

CHENG T., FISHER P.F., AND P. ROGERS. 2002. Fuzziness in multi-scale fuzzy

assignment of duneness. In G. Hunter and K. Lowell, editors, Accuracy 2002 - International Symposium On Spatial Accuracy Assessment in Natural Resources and Environmental Sciences, pages 154-159, Melbourne, Australia, July 10-12 2002.

CHENG, T. AND M. MOLENAAR. 2001. Formalizing fuzzy objects from uncertain classification results. *International Journal of Geographical Information Science*, 15(1):27-42.

FISHER, P.F. 2002. Fuzziness in multi-scale analysis of landscape morphometry. Personal Communication, October 2002.

FISHER, P.F. 1999. Geographical Information Systems: Vol. 1 Principles and Technical Issues, Vol. 2 Management Issues and Applications, chapter Models of Uncertainty in Spatial Data, pages 191-205. Wiley & Sons, New York, second edition edition, 1999.

FOODY, G. M. 1996. Approaches for the production and evaluation of fuzzy land cover classifications from remotely sensed data. *International Journal of Remote Sensing*, 17(1):1317-1340.

GORTE, B. H. H. AND A. STEIN. 1998. Bayesian classification and class area estimation of satellite images using stratification. *IEEE Trans. Geosciences and Remote Sensing*, vol. 36, pp. 803–812.

HARALICK R.M., SHANMUGAM K., AND I. DINSTEIN. 1973. Textural features for image classification. *IEEE Transactions on Systems, Man and Cybernetics*, vol 2, pp. 610-621.

HARALICK R.M. AND L.G. SHAPIRO. 1985. Image segmentation techniques. *Computer Vision, Graphics and Image Processing*, 29(1):100-132.

HOOTSMANS R.M. 1996. Fuzzy Sets and Series analysis for Visual Decision Support in Spatial Data Exploration. PhD thesis, Utrecht University.

HOROWITZ S.L. AND T. PAVLIDIS. 1976. Picture segmentation by a tree traversal algorithm. Journal of the Association for Computing Machinery, 23:368-388.

LUCIEER, A. AND A. STEIN. 2002. Existential uncertainty of spatial objects segmented from remotely sensed imagery. *IEEE Transactions on Geoscience and Remote Sensing*, 40(11): 2518- 2521.

NIXON, M.S. AND A.S. AGUADO. 2002. Feature extraction & image processing. Butterworth-Heinemann.

OJALA T., PIETIKÄINEN M. AND D. HARWOOD. 1996. A comparative study of texture measures with classification based on feature distributions. *Pattern Recognition*,29: 51-59.

OJALA T. AND M. PIETIKÄINEN. 1999. Unsupervised texture segmentation using feature distributions. *Pattern Recognition*, 32: 477-486.

OJALA T., PIETIKÄINEN M., AND T. MÄENPÄÄ. 2002. Multiresolution gray-scale and rotation invariant texture classification with local binary patterns. *IEEE Transactions on Pattern Analysis and Machine Intelligence*, 24(7): 971-987.

PIETIKÄINEN M., OJALA T., AND Z. XU. 2000. Rotation-invariant texture classification using feature distributions. *Pattern Recognition*, 33:43-52.

RANDEN, T. AND J.H. HUSOY. 1999. Filtering for Texture Classification: A Comparative Study. *IEEE Transactions on Pattern Analysis and Macine Intelligence*, 21(4): 291-310.

SOKAL, R.R. AND F.J. ROHLF. 1987. Introduction to Biostatistics, 2nd edition. W.H. Freeman and Co, New York.

Texture Analysis, University of Oulu, Finland. 2003.
Website http://www.ee.oulu.fi/research/imag/texture/. Last accessed: 14 February 2003.

WEL, F. VAN DER. 2000. Assessment and Visualisation of Uncertainty in Remote Sensing Land Cover Classifications. PhD thesis, Utrecht University.

ZHANG J. AND G. M. FOODY. 2001. Fully-fuzzy supervised classification of sub-urban land cover from remotely sensed imagery: Statistical and artificial neural network approaches. *International Journal of Remote Sensing*, 22(4):615-628.